Available online at www.sciencedirect.com

ScienceDirect

Solid State Communications 144 (2007) 437–440

solid state communications

www.elsevier.com/locate/ssc

Room temperature synthesis of nanoporous silica spheres and their formation mechanism

Sajo P. Naik[a], Igor Sokolov[a,b,c,*]

[a] Department of Physics, Clarkson University, Potsdam, NY, 13699-5820, USA
[b] Department of Chemistry, Clarkson University, Potsdam, NY, 13699-5820, USA
[c] Center for Advanced Material Processing (CAMP), Clarkson University, Potsdam, NY, 13699-5820, USA

Received 19 August 2007; accepted 20 September 2007 by J.F. Sadoc
Available online 4 October 2007

Abstract

We describe a robust process for the synthesis of micrometer-sized nanoporous (mesoporous) silica spheres using disodium trioxosilicate as an economical silica source and cetyltrimethylammonium chloride as the structure directing agent by the self-assembly process in the presence of formamide under alkaline condition at room temperature. The surface area of the spheres is 600 m^2/g, whereas the pore diameter and pore volume are 3.3 nm, and 0.3 cm^3/g, respectively. The formation mechanism of the spheres is studied with dynamic light scattering (DLS) and atomic force microscopy (AFM) techniques. We found that the formation involved two steps. In the first step 20–30 nm size primary particles are formed which then fuse together in the second step to form micron-sized mesoporous spheres.

PACS: 81.16.Dn; 81.16.Be; 07.79.Lh; 81.07.-b

Keywords: A. Nanostructures; B. Chemical synthesis; C. X-ray scattering

1. Introduction

The synthesis of M41S family of nanoporous (mesoporous in another classification) silica [1–3] has generated a lot of research interest because of its potential applications as adsorbents, catalysts, ultrafiltration media, and as hosts for nanosized particles. Mesoporous silica was first synthesized in the beginning of 1990s by the self-assembly of polymeric silica together with ionic surfactants under basic conditions. So far, mesoporous silica in various morphological forms, such as powder [1–3], monolith [4], films [5] as well as particles in the morphologies of fibers [6–10], rods [9], gyroids/discoids [6,7] and spheres [11–14] can be synthesized under different processing conditions using alkyl orthosilicates as a silica source together with a structure directing agent (SDA). In addition, mesoporous silica in various structures such as hexagonal, cubic or lamellar, with varying pore diameters could also be tailor-made expanding its scope in a number of applications.

It should be noted that alkyl orthosilicates are generally used as a source of silica together with surfactants as an SDA for the preparation of mesoporous silica. However, they are not the best commercial sources of silica due to their high cost, flammability, and difficulties in handling/storage. Therefore, their replacement by comparatively less expensive and robust inorganic silica sources is much desired [15]. The utility of sodium silicate for the synthesis of mesoporous silica powders under hydrothermal conditions has already been demonstrated previously [16–18]; but the control of the morphology of well-formed mesoporous silica particles under a range of synthesis conditions is greatly desired. Previously, under acidic condition and using triblock copolymers [19] or mixture of surfactants [20], the synthesis of mesoporous silica spheres of 130–225 μm and 1–3.5 μm size, respectively, has been reported.

In this work, we report the synthesis of 6 μm average size mesoporous silica particles under alkaline synthesis condition and at room temperature in a fast and robust synthesis using disodium trioxosilicate ($Na_2SiO_3{\cdot}9H_2O$) as

---

* Corresponding author at: Department of Physics, Clarkson University, Potsdam, NY, 13699-5820, USA. Tel.: +1 315 268 2375; fax: +1 315 268 6610.
E-mail address: isokolov@clarkson.edu (I. Sokolov).

0038-1098/$ - see front matter © 2007 Elsevier Ltd. All rights reserved.
doi:10.1016/j.ssc.2007.09.033

silica source, and cetyltrimethylammonium chloride (CTAC) as an SDA. Furthermore, we investigate the mechanism of sphere formation using dynamic light scattering (DLS) and atomic force microscopy (AFM) techniques.

2. Experimental methods

2.1. Materials and synthesis

Mesoporous silica spheres were synthesized using $Na_2SiO_3 \cdot 9H_2O$ (Fischer Scientific) as the silica source, CTAC (aqueous 25%, Aldrich) as an SDA in the presence of formamide ($HCONH_2$, Aldrich) and hydrochloric acid (37%, J T Baker). The molar composition of the sol was maintained at 1 $Na_2SiO_3 \cdot 9H_2O$: 22 $HCONH_2$: 0.6 CTAC: 210H_2O.

At first $Na_2SiO_3 \cdot 9H_2O$ was dissolved in distilled water taken in a high density polyethylene (HDPE) bottle under stirring. CTAC solution was then added to the clear sodium silicate solution, followed by the addition of formamide at room temperature (25 °C). The stirring was continued for another 5 min and the resulting clear sol, pH 12, was maintained under quiescent conditions at 25 °C. After about 5 min from mixing, turbidity began to appear in the clear solution, the reaction mixture was maintained 25 °C for 3 h to complete the formation of spheres. The white product formed was collected by filtration, washed with copious amounts of water and air dried. The organics were removed by calcination at 400 °C in air.

2.2. Characterization

The powder X-ray diffraction (XRD) patterns on the as-synthesized materials were collected on an M03X-HF (Bruker AXS) instrument using Cu Kα radiation (40 kV, 40 mA). The scanning electron microscopy (SEM) images were taken on a JEOL 6300 instrument operating at 15 kV. Prior to the measurements, the samples were coated with gold for 1 min in an Anatech hummer 6.2 sputtering system operating at 40 millitorr. The transmission electron microscopic (TEM) images of the calcined particles were recorded on a JEM 2010 electron microscope (JEOL) at an acceleration voltage of 200 kV. The samples were prepared by dispersing the calcined material in water at room temperature. A few drops of this dispersion was placed on a holey carbon-coated mesh and dried at room temperature. The N_2 adsorption/desorption isotherms of the calcined mesoporous silica samples were measured at 77 K on a NOVA 1200e instrument (Quantachrome Co.). Before the measurement, samples were degassed at 350 °C and 10 Pa for at least 12 h. Dynamic light scattering (DLS) measurements on the sol were performed using BIC, 90 plus particle size analyzer at 25 °C. The particle size was evaluated using Brookhaven 90 plus particle size software and lognormal-intensity measurements were used to calculate the average particle size.

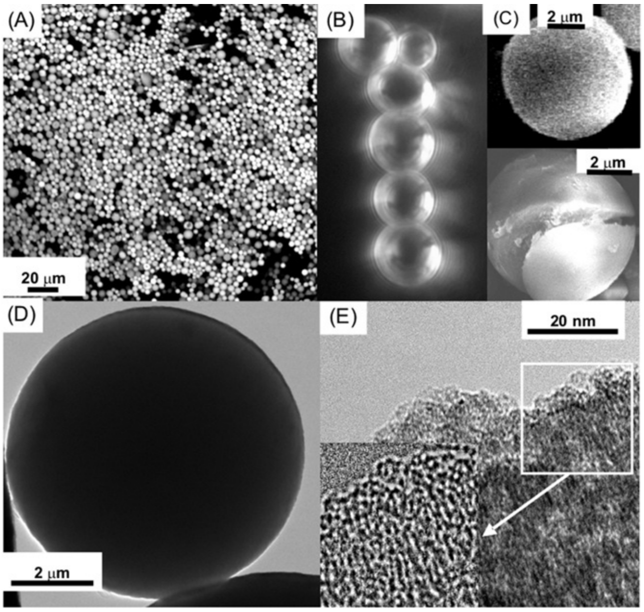

Fig. 1. CLSM (A) image, and dark-field optical (B) image (30 × 15 μm^2) of the as-synthesized spheres. (C) SEM images of individual spheres. Bottom image shows a rare event of broken sphere after calcination (D). TEM images of the spheres (E). The insert in (E) is a contract-enhanced part of the image. The spheres were synthesized from the sol of molar composition 1 $Na_2SiO_3 \cdot 9H_2O$:22 $HCONH_2$:0.6 CTAC:210H_2O at 25 °C, 3 h.

The atomic force microscope (AFM) used in this study was a Dimension 3100 Nanoscope AFM (DI/Veeco, CA) with built-in video optical system. The AFM was operated in taping mode in ambient conditions. Oxygen sharpened AFM probes, RESP (Veeco/Digital Instruments, CA) were used in this study. The AFM software v.5.12r4 was employed. The spheres for imaging were dispersed over semi-rigidified epoxy. After the epoxy curing, the excess of the particles was removed by blowing with air. The area for imaging was located by using built-in optical system.

3. Results and discussion

The yield of the obtained mesoporous spheres was high, above 90%, on the basis of the silica recovery. The images of the mesoporous silica spheres are shown in Fig. 1. The spheres are hard and the combined, CLSM, optical and TEM, studies provided concrete proof for their dense internal morphology [Fig. 1(B)–(D)]. There was no change in the external morphology of the spheres after calcination except that a few spheres were found to be broken [Fig. 1(C)]. Although the spheres are hard, they have a wormhole-like mesoporous internal structure as found from the high resolution TEM image shown in Fig. 1(E). The mesopores in the spheres are open from the external surface and provide pore accessibility to the external species, molecules and nanoparticles of appropriate size.

The presence of bulk ordered mesostructure was further confirmed from XRD pattern of the spheres shown in Fig. 2. The mesoporosity was further confirmed from the N_2 adsorption/desorption measurement conducted at 77.3 K on the calcined spheres, shown in Fig. 3. The isotherm showed a step rise at 100 ∼ 0.2 P/P0 with a little hysteresis, typical of wormhole-like mesoporous materials. The pore size was estimated from the adsorption branch of the isotherm

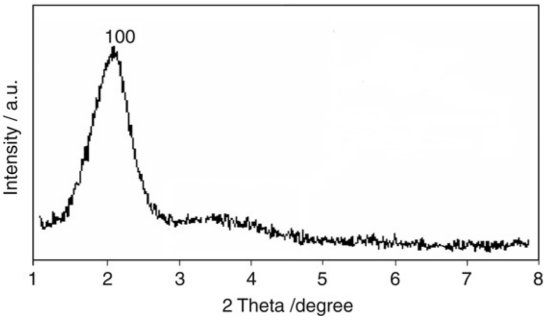

Fig. 2. XRD pattern of the synthesized mesoporous silica spheres.

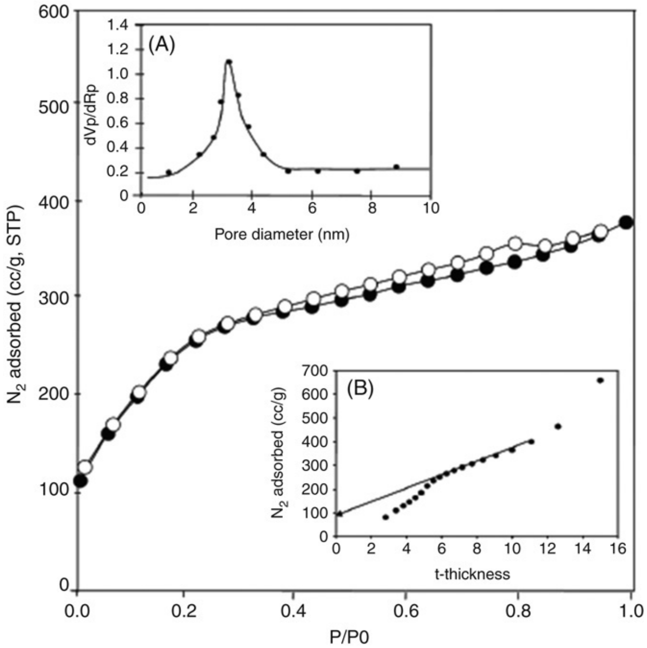

Fig. 3. N_2 adsorption/desorption isotherms obtained on calcined mesoporous silica spheres at 77.4 K. Insets (A) pore size distribution (B) *t*-plot.

according to the correlation obtained from NLDFT theory [21,22]. The BET surface area of the spheres was 600 m^2/g, whereas the mesopore diameter and pore volume were 3.3 nm, and 0.3 cm^3/g, respectively. Pore size distribution and *t*-plot analysis are shown as insets in Fig. 3, there was no presence of micropores in the material.

It should be noted that the spheres could not be formed in absence of formamide in the synthesis sol, the amount of formamide also influenced the morphology of the spheres dramatically. For example, doubling the amount of formamide decreased the average diameter of the spheres by $\sim$2 μm. Previously, Zhao et al. [23] proposed that polar cosolvents such as *N*, *N*-dimethylformamide can interact with amphiphilic block copolymer, SDA, resulting in the lowering of local curvature energy of the silica/SDA mesophase, thus explaining the role of formamide in the formation of spheres in our study. In another study, it was also shown that the shape of hexagonal mesoporous silica particles is determined in part by the free energy of silicified nematic mesophase [7,24,25], therefore, lowering the local micelle curvature keeps the mesoporous shape of the morphology on the same energy level (with respect to the surface energy), hence, allowing them to exist in the synthesis product. Therefore it is plausible to expect formamide-CTAC interaction leading to a decrease in the curvature of SiO_2/CTAC mesophase due to specific location of formaldehyde molecules and forwarding the formation of spherical shape silica.

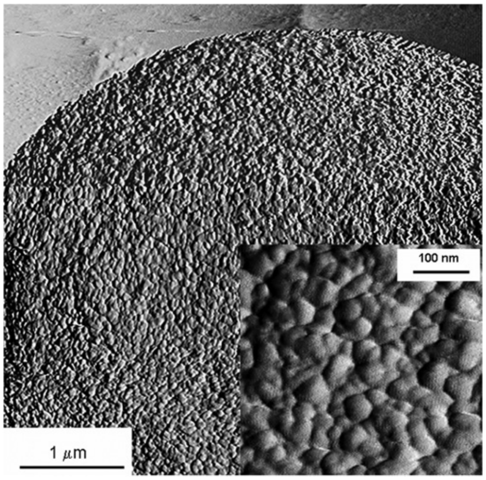

Fig. 4. An AFM image showing the surface of the synthesized mesoporous silica spheres. Inset shows a zoom scan.

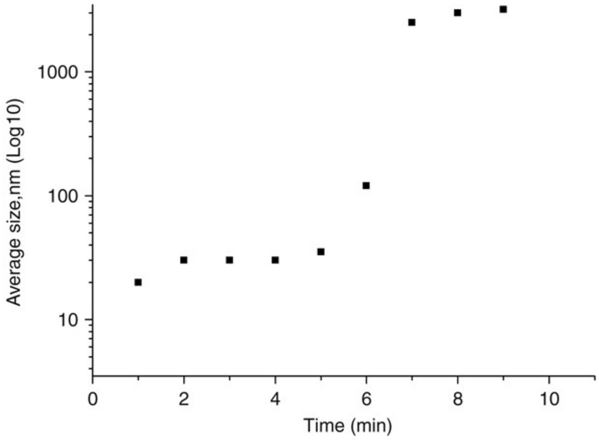

Fig. 5. The growth of spherical mesoporous silica spheres followed by using DLS technique.

We further investigated the formation mechanism of the spheres using AFM and DLS techniques. AFM image (Fig. 4) of the external surface of the spheres presents a granular-type structure. This indicates the sphere formation, at least at the last stage, by the aggregation of smaller nanosize subunits or primary particles. A higher magnification AFM image (inset in Fig. 4) demonstrates that the exterior surfaces of these particles are formed by the aggregation of subunits of 20–30 nm in size. We followed the growth of mesoporous silica spheres using DLS technique; the DLS plot of size of the growing particles in Fig. 5 shows two stages during particle formation. The first is the formation of the primary particles in the clear sol that lasts for about five minutes from the starting of the reaction. After that, a rapid growth is initiated, which is leading to the formation of larger particles, the observed spheres. The sol at this stage becomes turbid with a concomitant increase in the size of the particles, Fig. 5. It should be noted here that to do the DLS measurements for thick precipitates, the samples had to be diluted with water so as to be within the concentrations suitable for DLS measurements and avoid multiple scatterings. The size of the particles at the initial stage observed from DLS is close to that of smaller subunits observed with AFM. This makes it plausible to conclude that the 20–30 nm primary particles are the building blocks of the micrometer-sized particles aggregating to form larger spheres. Mesoporous silica spheres synthesized using tetraethyl alkoxide show similar pattern in DLS during their growth in acidic or basic conditions [26,27]. We will study the universality of this step of the formation mechanism in our future works.

4. Conclusions

We have described a robust process for the synthesis of micrometer-sized mesoporous silica spheres. The spheres are synthesized under alkaline conditions and at room temperature in a short time using disodium trioxosilicate as an economical silica source and cetyltrimethylammonium chloride as the structure directing agent through the self-assembly process. The BET surface area of the spheres was 600 m^2/g, whereas the mesopore diameter and pore volume were 3.3 nm, and 0.3 cm^3/g, respectively.

Here we have conclusively established the presence of primary particles of 20–30 nm in size, by AFM and DLS techniques, during the short incubation period of the reaction. The primary particles then self-assemble into well-organized spheres in the second step of the reaction.

Acknowledgment

Financial support from the ARO (grant W911NF-05-1-0339) is acknowledged.

References

[1] T. Yanagisawa, T. Shimizu, K. Kuroda, C. Kato, Bull. Chem. Soc. Jpn. 63 (4) (1990) 988.
[2] C.T. Kresge, M.E. Leonowicz, W.J. Roth, J.C. Vartuli, J.S. Beck, Nature 710 (1992) 6397.
[3] J.S. Beck, J.C. Vartuli, W.J. Roth, M.E. Leonowicz, C.T. Kresge, K.D. Schmitt, C.T.W. Chu, D.H. Olson, E.W. Sheppard, S.B. Mc Cullen, J.B. Higgins, J.L. Schlenker, J. Am. Chem. Soc. 114 (1992) 10834.
[4] H. Yang, Q. Shi, B. Tan, S. Xie, F. Zhang, Y. Yan, B. Tu, D. Zhao, Chem. Mater. 15 (2003) 536.
[5] M. Ogawa, J. Am. Chem. Soc. 116 (1994) 7941.
[6] H. Yang, N. Coombs, G.A. Ozin, Nature 386 (1997) 692.
[7] I. Sokolov, Y. Kievsky, Stud. Surf. Sci. Catal. 156 (2005) 433.
[8] Y. Kievsky, I. Sokolov, IEEE Trans. Nanotech. 4 (2005) 490.
[9] G.A. Ozin, H. Yang, I. Sokolov, N. Coombs, Adv. Mater. 9 (1997) 662.
[10] Q. Huo, D. Zhao, J. Feng, K. Weston, S.K. Buratto, G.D. Stucky, S. Schacht, F. Schuth, Adv. Mater. 9 (1997) 974.
[11] S. Schacht, Q. Hou, I.G. Voigt-Martin, G.D. Stucky, F. Schüth, Science 273 (1996) 768.
[12] Q. Huo, J. Feng, F. Schüth, G.D. Stucky, Chem. Mater. 9 (1997) 14.
[13] H. Yang, G. Vovk, N. Coombs, I. Sokolov, G.A. Ozin, J. Mater. Chem. 8 (1997) 743.
[14] D. Zhao, J. Feng, Q. Huo, N. Melosh, G.H. Fredrickson, B.F. Chmelka, G.D. Stucky, Science 279 (1998) 548.
[15] A. Berggren, A.E.C. Palmqvist, K. Holmberg, Soft Matter. 1 (2005) 219.
[16] L. Sierra, B. Lopez, H. Gil, J.-L. Guth, Adv. Mater. 11 (1999) 307.
[17] L. Sierra, J.-L. Guth, Microporous Mesoporous Mater. 27 (1999) 243.
[18] J.M. Kim, G.D. Stucky, Chem. Commun. (2000) 1159.
[19] K. Kosuge, N. Kikukawa, M. Takemori, Chem. Mater. 16 (2004) 4181.
[20] X. Pang, F. Tang, Microporous Mesoporous Mater. 85 (2005) 1.
[21] A.V. Neimark, P.I. Ravvikovitch, Microporous Mesoporous Mater. 44 (2001) 697.
[22] M. Jaroniec, M. Kruck, J.P. Olievier, Langmuir 15 (1999) 5410.
[23] D. Zhao, J. Sun, Q. Li, G.D. Stucky, Chem. Mater. 12 (2000) 275.
[24] I. Sokolov, H. Yang, G.A. Ozin, C.T. Kresge, Adv. Mater. 11 (1999) 636.
[25] M. Ogura, H. Miyoshi, S.P. Naik, T. Okubo, J. Am. Chem. Soc. 126 (35) (2004) 10937.
[26] K. Yano, Y. Fukushima, J. Mater. Chem. 14 (2004) 1579.
[27] H. Yang, G. Vovk, N. Coombs, I. Sokolov, G.A. Ozin, J. Mat. Chem. 8 (1998) 743.